



# Objective method for measuring the macular pigment optical density in the eye

DIMITRIOS CHRISTARAS,<sup>1,2,\*</sup> HARILAOS GINIS,<sup>2</sup> ALEXANDROS PENNOS,<sup>1</sup> JUAN MOMPEAN,<sup>1</sup> AND PABLO ARTAL<sup>1</sup>

<sup>1</sup>Laboratorio de Óptica, Instituto Universitario de Investigación en Óptica y Nanofísica, Universidad de Murcia, Campus de Espinardo, E-30100 Murcia, Spain

<sup>2</sup>Department of Research, Athens Eye Hospital, Leof. Vouliagmenis 45, Glifada 166 75, Greece

\*dimitrios@um.es

**Abstract:** Macular pigment is a yellowish pigment of purely dietary origin, which is thought to have a protective role in the retina. Recently, it was linked to age-related macular degeneration and improved visual function. In this work, we present a method and a corresponding optical instrument for the rapid measurement of its optical density. The method is based on fundus reflectometry and features a photodetector for the measurement of reflectance at different wavelengths and retinal locations. The method has been tested against a commercially available instrument on a group of healthy volunteers and has shown good correlation. The proposed instrument can serve as a rapid, non-midriatic, low-cost tool for the measurement of macular pigment optical density.

© 2019 Optical Society of America under the terms of the [OSA Open Access Publishing Agreement](#)

## 1. Introduction

Macular Pigment (MP) is a collective term for the carotenoids lutein, zeaxanthin and meso-zeaxanthin. The pigment is found mainly -but not exclusively- at the macula, with higher concentration observed usually at the centre of the fovea [1]. Macular pigment's role is believed to be twofold: on the one hand it acts as a long-pass filter, protecting the foveal photoreceptors from photochemical damage due to short-wavelength light [1]; on the other hand, it is an anti-oxidant protective agent quenching the toxic by-products of the visual cycle [2]. Also, a study has shown that lutein due to its anti-inflammatory action can prevent choroidal neovascularisation [3]. Recent findings suggest that the optical density of macular pigment is significantly lower in case of degenerative macular diseases such as age-related macular degeneration (AMD) [4, 5], further supporting the protective hypothesis. Macular pigment has also been related to visual function; studies suggest that higher density is linked to improved visual performance, particularly acuity [6, 7]. Finally, recent studies have also seen a relation between the MP distribution and macular telangiectasia type 2 [8, 9].

The in-vivo assessment of MP can be done either through psychophysical methods, such as Heterochromatic Flicker Photometry (HFP) [10–13] and minimal motion photometry [14], or optical methods, such as fundus reflectometry [15–18], autofluorescence [19] and Raman spectroscopy [20]. Currently, the most commonly used method in clinical practice for the measurement of the Macular Pigment Optical Density (MPOD) is based on HFP, a method originally used to measure the spectral sensitivity of the human visual system. Macular pigment can be assessed by estimating the blue/green sensitivity separately at the fovea and the periphery; the main assumption is that MP absorbs solely at shorter wavelengths and it is located mainly at the fovea, and therefore any difference at the spectral sensitivity between the two retinal locations can be attributed to MP. Subjects with higher MPOD would, therefore, perceive less blue light at the fovea than at the periphery than subjects with lower MPOD. Although the method has shown a good repeatability [21–23], it can be time-consuming and the task required by the patient is not trivial and often difficult for some subjects to perform. The optical methods for the assessment

of MPOD require less time and are more accurate than the psychophysical ones in general, but they usually require high-end components, they are bulky and costly instruments that perform complex post-processing of the images that often make them impractical for wide clinical use.

In this work, we present an objective, non-invasive system capable of measuring the MPOD rapidly, accurately and without the need of pupil dilation, apt for wide clinical use. The key element behind this method is that the spatial information needed for the calculation of MPOD can be coded in the illumination path, allowing us to replace the camera sensor which is traditionally used in this kind of systems, with a high-speed, high sensitivity photo-detector. The use of a photodetector can lead to a much faster and less noisy measurement of the MPOD that requires minimum retinal light exposure. Additionally, it decreases significantly the complexity and the cost of the system, setting the grounds for a cheap, compact device for the rapid measurement of macular pigment optical density.

## 2. Methods

### 2.1. Optical system

The optical system (see Fig. 1) is based on the double-pass principle [24]. The illumination of the fundus is done using LED sources of two different wavelengths, merged using a cold mirror and collimated using a lens (L1). Light is then guided to the pupil through a relay telescope (L2 & L3) and focuses on the subject's retina. The reflected retinal light is then guided through the same relay telescope and a half mirror (HM) to a silicon photomultiplier (SiPM) device (Excelitas, Waltham, MA, USA). A flip mirror redirects the beam to a CMOS monochrome camera (FLIR Systems, Inc., Richmond, BC, Canada), turning the system into a fundus camera, at will. A tunable lens (EL-10-30, Optotune, Switzerland) was introduced in the camera's path to compensate for defocus in non-emmetropic subjects and chromatic defocus.

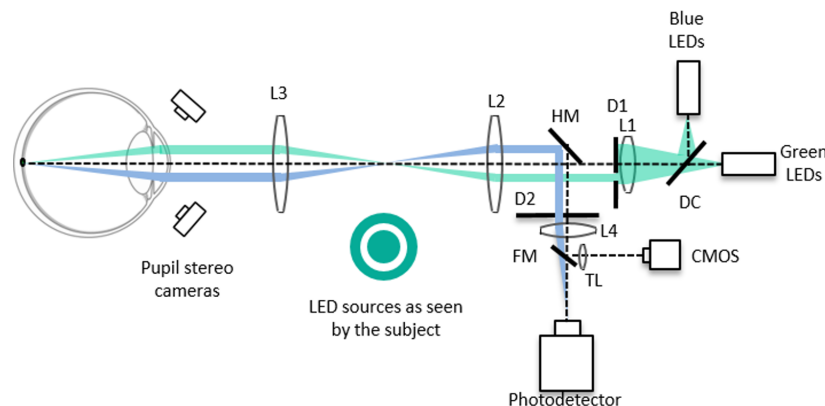


Fig. 1. Schematic of the Optical system.

The two arms (illumination and imaging) are separated using appropriate offset diaphragms (D1 & D2), both conjugated to the pupil plane through the relay formed by lenses L1 and L2. Diaphragm D1 was chosen to be less than 2mm wide at the pupil plane, so that the field on the retina remained constant in size, for non-emmetropes as well. The relative separation of the two diaphragms at the pupil plane was determined through simulations using an optical design software (Zemax LLC, WA, USA), which were based on geometrical and optical values for the average eye [25]. This configuration ensured that all back-reflected light from the cornea or the lens did not reach the detector. A similar entrance/exit diaphragm configuration to avoid back-reflections has been used in previous systems by our group [18, 26–29].

The alignment of the pupil is done using a stereoscopic system that permits very high axial resolution. A detailed description of the stereo pupil system can be found elsewhere [30, 31]. Specular reflections from lenses L2 and L3 (see Fig. 1) are avoided by lightly tilting them ( $5^\circ$ )

The illumination consists of four LED sources, that each one is driven at a distinct frequency. The four LED sources (see Fig. 1) are arranged spatially and spectrally as follows: two of the LEDs, are disk-shaped with peak emission at 450nm and 550nm respectively, and the other two LEDs are annular-shaped, concentric to the disk, with peak emission at 450nm and 550nm respectively. The disk-shaped sources are 3.5 degrees in diameter and the annular sources are of 1 degree thickness and an inner radius of about 5.5 degrees. The disks illuminate the central part of the retina and the annuli illuminate the peripheral part of the retina, where blue light absorption due to MPOD is maximum and minimum respectively. The flicker frequencies for the four LED sources were as follows: 450 Hz for the green central disk, 350Hz for the blue central disk, 500Hz for the green annulus and 400Hz for the blue annulus. The total exposure time was 0.27s, roughly the reaction time of the pupil, making the measurement non-midriatic. The subject's fixation is done using a dim red LED source projected through the green channel.

The two independent light sensors, i.e. the photodetector and the CMOS camera, can be used sequentially through a flip mirror. Only the photodetector is used for the MPOD measurement however; the CMOS camera is solely used to collect spatial information for validation purposes, i.e. to check for possible specular reflections in the system from the optics or the fundus and to use the spatial information from the fundus images in order to determine the appropriate size for the central and the peripheral field. For the measurement using the CMOS camera, the LED sources flash sequentially, one wavelength at a time. Four images were acquired at each wavelength which were then registered and averaged using an image processing software (ImageJ) to increase the signal-to-noise ratio. All eight images were captured within 0.25 seconds in order to avoid provoking the pupil reflex. The exposure time of each image was kept at about 20ms per image. The focus between the two wavelengths was changed using the tunable lens (see TL in Fig. 1) in order to compensate for the chromatic defocus of the eye and for defocus in non-emmetropic volunteers. The initial focus was found via a through-focus process where the best focus was determined at each wavelength.

## 2.2. Signal processing and macular pigment optical density calculation

The captured signal is the sum of four distinct signals originating from the two different retinal locations (disk and annulus) at two different wavelengths (blue and green). Each signal flickers at a distinct temporal frequency. An example of a 0.1s fraction of a signal from a real eye, in the time and frequency domain is depicted in Fig. 2.

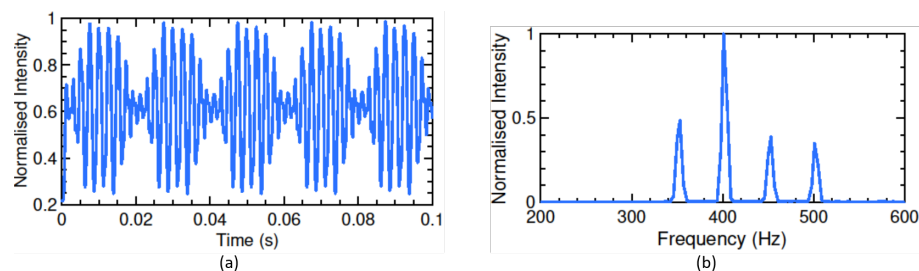


Fig. 2. (a) An example of a signal, captured by the photodetector (b) its Fourier Transform showing the four distinct peaks, corresponding to the four different frequencies.

In the standard reflectance method where a camera is used, the reflectance values of each camera pixel are measured at two wavelengths, blue and green, where the absorption is maximum

and minimum respectively. Let peripheral blue reflectance, peripheral green reflectance, central blue reflectance and central green reflectance be  $R_P^B$ ,  $R_P^G$ ,  $R_F^B$  and  $R_F^G$  respectively, then the MPOD will be given by the following generic formula

$$MPOD(r, \theta, 460) = \frac{0.5}{K_{MP}^B - K_{MP}^G} \left\{ \log_{10} \frac{\sum R_P^B}{\sum R_P^G} - \log_{10} \frac{R_F^G(r, \theta)}{R_F^B(r, \theta)} \right\}. \quad (1)$$

where  $K_{MP}^B$ ,  $K_{MP}^G$  the extinction coefficients of Macular Pigment, normalised at 460nm, for blue and green respectively,  $r$  the radial coordinate in degrees of visual angle and  $\theta$  the angular coordinate. For the peripheral values, instead of a single point, a small retinal region is considered, denoted by the sum in the formula. The derivation of the above formula can be found in detail elsewhere [18, 19].

Equation (1) gives a complete spatial description of the MPOD at the retina. This, however, can be highly impractical in clinical practice. Although there is not a single standard metric, in order to give some clinical relevance to the measurement, an average of the central MP area is usually calculated and used as the MPOD value associated to the subject. In our proposed method, the reflectance values measured by the photodetector are the total reflectance of the central 3.5-degree area and the 1-degree peripheral annulus at the two wavelengths. Equation (1) then becomes

$$MPOD(460) = \frac{0.5}{K_{MP}^B - K_{MP}^G} \left\{ \log_{10} \frac{\sum R_P^B}{\sum R_P^G} - \log_{10} \frac{\sum_{r=0^\circ}^{1.75^\circ} \sum_{\theta=0}^{2\pi} R_F^G(r, \theta)}{\sum_{r=0^\circ}^{1.75^\circ} \sum_{\theta=0}^{2\pi} R_F^B(r, \theta)} \right\}. \quad (2)$$

The extinction coefficients  $K_{MP}^B$ ,  $K_{MP}^G$  were calculated during calibration. Equation (2) returns a single number for MPOD, which is an average value for the central area.

### 2.3. Calibration

The system was calibrated using a filter (DI8, Noir LaserShields, South Lyon, MI, USA) with known optical density of 1 D.U. and spectral absorption very similar to macular pigment. The filter was mounted at the center of a surface of spectrally and spatially uniform reflectance was used to simulate the ocular fundus with MPOD equal to 1. The filter was then removed to simulate a fundus with MPOD equal to 0. The total power of the LED sources at the retina was  $75\mu W$ , well below the maximum permissible exposure for ocular safety for the exposure time of the measurement [32].

### 2.4. Volunteers

Thirteen volunteers with no known ocular disease participated in this study, with a mean age of 32.5 years old (STD 8.7). All measurements followed the tenets of the Declaration of Helsinki and were approved by the local ethics committee. Informed consent was obtained from the subjects after they were fully informed about the nature of the measurements.

## 3. Results

### 3.1. Spatial reconstruction of macular pigment

Fundus images for three subjects were taken at the two wavelengths using the system's CMOS camera. An example of two fundus images for the same subject at the two wavelengths is shown in Figs. 3(a) and 3(b) for green and blue respectively.

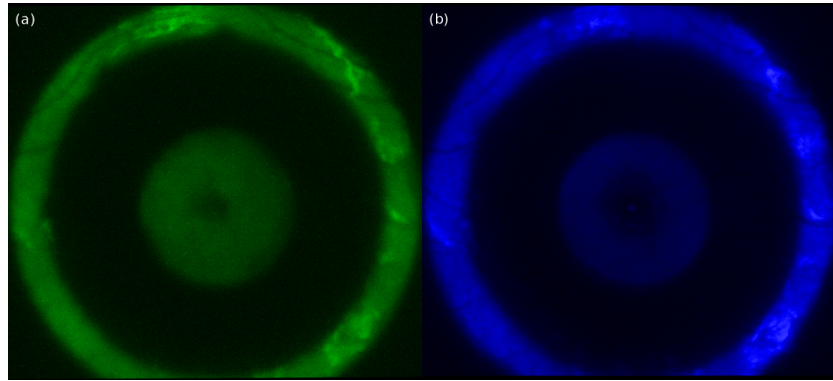


Fig. 3. Fundus image at green (left) and at blue (right) using the instrument's CMOS monochrome camera. The colouring of the images was at post processing to highlight the difference.

The pixel intensity values obtained from the fundus images were subsequently plugged into the following formula:

$$MPOD^*(\theta_x, \theta_y) = \log_{10} \frac{R_F^G(\theta_x, \theta_y)}{R_F^B(\theta_x, \theta_y)}. \quad (3)$$

where the  $\theta_x$ ,  $\theta_y$  the distance from the center of the fovea in degrees of visual angle, and  $R_F^G$ ,  $R_F^B$  the measured pixel intensity at green and blue respectively. Equation (3) gives the non-normalised spatial distribution of MPOD in the retina, i.e. the value of MPOD is given in arbitrary units. In order to differentiate this value from the quantitative MPOD measurement using the Fourier method, the non-normalised MPOD value was denoted with a star. The spatial distributions for two of the volunteers are shown in Figs. 4(a) and 4(b). The  $x$  and  $y$  axis of the figures are

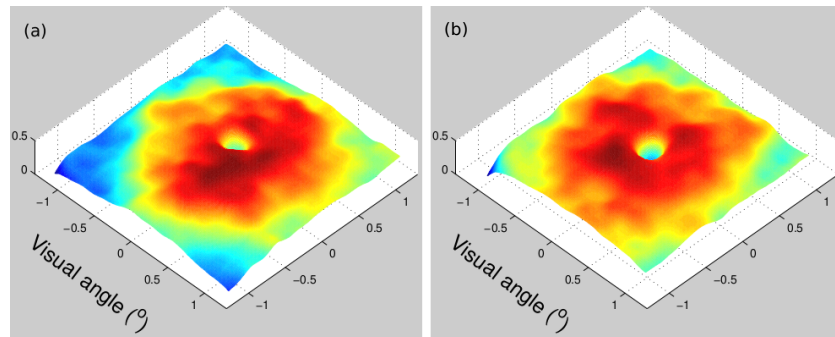


Fig. 4. Spatial reconstruction of MPOD for two subjects.

expressed in degrees of visual angle, centered around the fovea. A Gaussian smoothing was applied to the images prior to the spatial reconstruction of MPOD in order to reduce noise.

### 3.2. MPOD measurements and repeatability

The MPOD was calculated using the method described in section 2.2 for both eyes of 13 volunteers. The value was the average of three consecutive measurements. Each volunteer was instructed to fixate at the centre of the test field and was aligned using the stereo pupil camera system. Each measurement lasted 0.27 seconds and the volunteer lost fixation and was re-aligned

between measurements. The whole process (three measurements and alignment) lasted less than two minutes in total. Each volunteer was, then, associated with a mean value and a standard deviation. The results for both eyes are shown in Fig. 5. The average MPOD of all 13 subjects

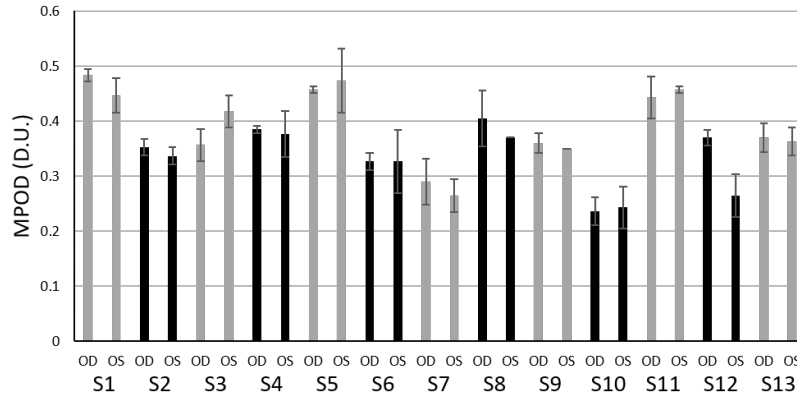


Fig. 5. MPOD value for right and right eye for each of the thirteen subjects. The depicted value is the mean from three consecutive measurements and the error is given by the standard deviation.

(26 eyes) was found to be  $0.37 \pm 0.07$ D.U..

In order to investigate the repeatability of the instrument, the agreement between the first and the second measurement on each subject was tested using the Bland-Altman (BA) analysis. The BA method focuses in the quantification of the difference between the two measurements, instead of the (obvious) correlation. The analysis consists of calculating the mean value of the differences (bias) of the measurement as well as the limits of agreement (LoA), defined as the mean difference  $\pm 1.96$  times the standard deviation of differences. The result of the (BA) analysis for the test-retest are shown in Fig. 6(a). The resulted bias was found to have a value of 0.004 and the limits of agreement were very narrow (0.05,-0.04), indicating a good repeatability of the instrument.

The right-left eye agreement was also investigated and the results of the BA analysis are shown in Fig. 6(b). The analysis has shown a bias of 0.011, upper limit of agreement 0.085 and lower

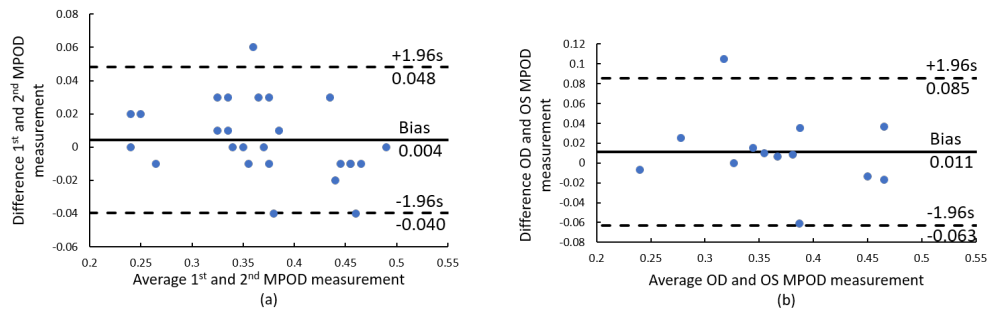


Fig. 6. (a) Bland-Altman plot for first and second measurement for the 13 volunteers (26 eyes), showing the repeatability of the proposed instrument. (b) Bland-Altman plot for right and left eye showing the agreement between right and left eye.

limit of agreement -0.063, indicating a good inter-eye agreement.



### 3.3. Comparison with MPSII

Currently, there are very few commercial devices that measure MPOD. A psychophysical instrument that is used in clinical practice is the MPS II (Elektron Technology; Cambridge, UK). It uses the Heterochromatic Flicker Photometry (HFP) method to determine the MPOD through the relative green to blue sensitivity of the visual system at the fovea. The instrument offers two test options: a standard and a detailed. The former is aimed for the general population and it is faster whereas the latter is suggested in cases of AMD or other retinal diseases that make the standard test difficult to perform. In our case all volunteers were tested using the standard test. Each measurement consisted of a first training test where the volunteers is guided through the experiment and their task is explained in detail. Subsequently, three measurements on each eye were carried out and the mean value was calculated. In case of an invalid measurement (indicated by the instrument's software) the measurement was repeated in order to have three acceptable measurements for each subject. A more detailed study in the repeatability of the instrument can be found in [21–23,33].

Three of the volunteers were unable to perform the test with the psychophysical instrument and one volunteer performed it only on their dominant eye. Therefore, the volunteer pool for the psychophysical measurement consisted of 10 volunteers or 19 eyes in total. The mean and the corresponding standard deviation for the above group of volunteers is shown in Fig. 7(a). The Bland-Altman plot for the first and second measurement using the psychophysical instrument is shown in Fig. 7(b). From the BA analysis shown in Fig.7(b) the instrument shows a mean

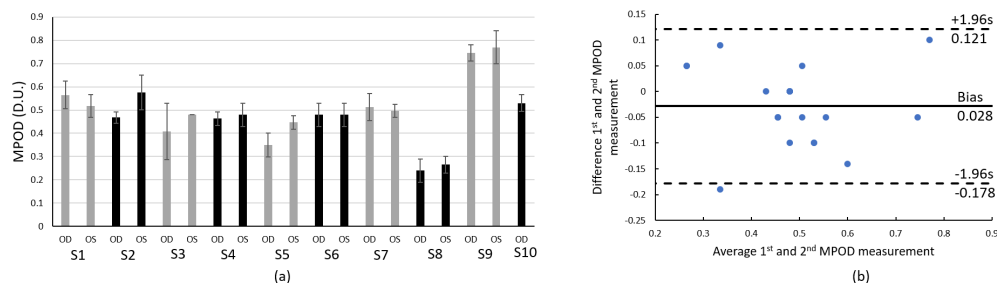


Fig. 7. (a) MPOD value for a total of 19 eyes using the psychophysical MPS II instrument. The value is the mean of three consecutive valid measurements and the error is given by the standard deviation. (b) Bland-Altman plot for first and second measurement for the 10 volunteers (19 eyes), showing the repeatability of the psychophysical MPS II instrument.

difference of 0.028 and upper and lower limits of agreement 0.121 and -0.178 respectively, similar to what a previous study for the same instrument has shown [21–23,33].

The average value of the MPOD for the volunteer pool using MPSII was found to be  $0.49 \pm 0.19$  D.U., significantly higher than the average value found using the proposed optical instrument. Compared with the proposed optical instrument, MPS II shows a lower repeatability for the specific group of volunteers.

In order to validate the proposed instrument, the correlation between the latter and the MPSII screener was tested, for the same sub-group of volunteers who were able to perform the psychophysical test. This is shown in Fig. 8. A regression analysis was carried out to investigate correlation between the two instruments for the given group of volunteers. The analysis has shown that the two set of measurements from the difference instrument are linearly related with R-square equal to 0.49 and p-value 0.00085. The regression coefficients mean that correlation is indeed significant ( $p < 0.005$ ) but the values show a relatively high scatter around the regression line ( $R^2 = 0.499$ ).

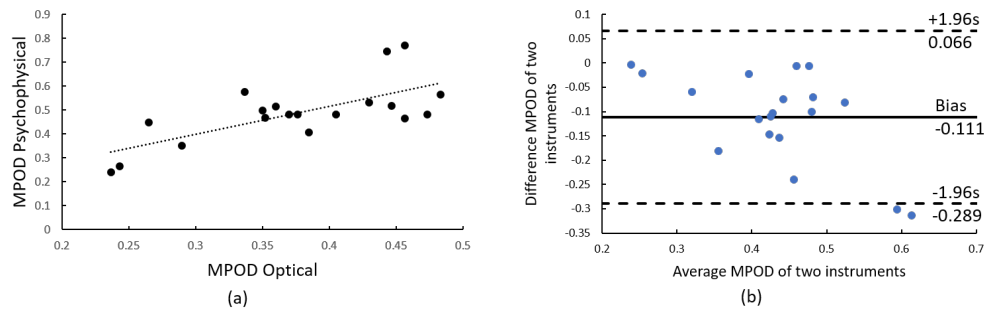


Fig. 8. (a) MPOD using our proposed optical method vs MPOD using the commercial psychophysical device MPS II for a total of 10 volunteers (19 eyes). The value in both cases is the mean of three consecutive measurements. (b) Bland-Altman plot, investigating the agreement between the two methods.

#### 4. Discussion

In this work, we propose an optical method and a corresponding instrument for the in-vivo measurement of the optical density of Macular Pigment, in a rapid, safe, accurate and potentially cost-effective way. In this novel method, the retina is illuminated with short pulses of structured light of different wavelengths and the signal is collected by a photodetector and analysed in the Fourier domain. The use of a high-speed, high-sensitivity photodetector allowed accurate and repeatable measurements in non-midriatic eyes. The illumination was done using high-power LED sources and the system featured only a few optical components, namely four singlet lenses, a cold mirror, a half-mirror and two diffusers. The optical instrument showed a high repeatability and also confirmed the high interocular correlation in MPOD, observed in previous studies.

There have been extensive discussions on the accuracy of both the psychophysical and the optical method and the extent to which the underlying assumptions are correct in each method. Heterochromatic Flicker Photometry is a method primarily used to measure the visual system's spectral sensitivity. The MPOD can then be derived using the measured spectral sensitivities, which is assumed to be the same at both retinal locations and, therefore, affected solely by attenuation due to macular pigment. This latter assumption, however, is not entirely accurate: a study by Sharpe et al [12] on spectral sensitivities in a deuteranope, a protanope and a normal trichromat under different cone isolation scenarios showed several discrepancies that could be due to the known photoreceptor optical density change with eccentricity or the presence of other shortwave absorbing retinal pigments with eccentricity dependence. Delori et al [19] in their work, concluded that the effect of the photopigment density differences (also known as self-screening) leads to an underestimation of 0.03-0.07D.U. for a photopigment optical density between the centre and periphery of 0.1-0.2D.U. Another factor that can possibly lead to a wrong estimation of MPOD when using HFP, is the relative sensitivities of the photoreceptors. This can be largely overcome, however, by favouring a single cone class. [12]

The fundus reflectometry method, on the other hand, makes the assumption that the ratio of fundus reflectance at the periphery and at the fovea is the same for both blue and green, save for macular pigment. It is, however, well-known that RPE's melanin density changes with eccentricity, usually exhibiting its maximum density at the fovea [34, 35]. This, in combination with melanin's higher absorption at lower wavelengths can render the latter assumption inaccurate and lead to an underestimation of MPOD, that would not be constant but it would depend on the individual's melanin difference between the two sites. Delori et al [19], after estimating the mean melanin density difference between the centre and the periphery for 172 subjects concluded that this difference accounts for a mean underestimation of 0.03D.U. in the MP optical density. In our



system, due to the larger area sampled, the underestimation in the MP density measurement due to melanin differences will be even lower.

The proposed instrument was optimised to accurately measure the amount of light reflected at the different retinal locations and at two different wavelengths using a high-sensitivity photodetector. Nevertheless, a low-cost CMOS camera was introduced to the system at a separate path, which allowed us to obtain retinal images at both wavelengths. The objective of the camera was twofold; first to check for any reflections prior to the ocular fundus or any other fundus anomalies, and second to check the extend of the spatial distribution of MP. The former is important in order to assure that light coming from the fundus is not contaminated by reflections prior to the fundus and that there are no structures that could alter the measurement; the spatial reconstruction of the MP, on the other hand, allowed to determine the appropriate field size of the central field and see the effect of eye movements during fixation. From preliminary qualitative spatial data for a set of subjects and based on the spatial distribution of MP from the literature [1], we concluded that a 3.5 degrees diameter central field would include the region of interest and any involuntary eye movements would not affect the computed value, since the greater part of the MP distribution would still be contained in the central field.

As mentioned previously, in our work, the CMOS sensor was only used to extract qualitative data. This was mainly due to the fact that the system was designed to use the minimum retinal illumination, while measuring through an undilated pupil. Therefore, for the given CMOS sensor and system configuration, it would require more light to achieve a reliable quantitative MPOD measurement.

The spatial distribution of the Macular Pigment has been a topic of study in the past, both ex-vivo [1] and in-vivo [16, 20, 36–39] using several different techniques. Although, it varies greatly among subjects, all studies come down to two main observations regarding the spatial distribution of the pigment: first, it is very steep in the first few degrees around the fovea and becomes practically undetectable at 6-7 degrees in the periphery, and second it can often show irregularities. In fact, Berendschot [40] et al have seen a ring-like distribution in approximately half of their subjects that appears at eccentricities between 0.5 and 1 degrees. Both observations on the spatial distribution of macular pigment are consistent with the distributions shown in Fig. 4. Both subjects showed a central dip in MPOD that is not necessarily a measurement artifact; previous studies have shown such central dips in subjects [41–43].

The spatial characteristics of the macular pigment are detrimental for the choice of the appropriate MP metric that would make sense in clinical practice. The measurement needs to be a single number that best describes the individual's MPOD in the retina. One for instance could choose the maximum value of the distribution; this, however, would fail to give an accurate picture of MPOD and it wouldn't reflect the actual MPOD value. Although there is no universal metric used in the measurement of MPOD, a commonly used metric is the mean of the MPOD the central few degrees. In our proposed method, we decided to gather the light of an area of 3.5 degrees. The field size was chosen such that on the one hand contains all the clinically important information for macular pigment and on the other hand minimises the impact of eye movements during fixation.

Both instruments, the proposed optical one and the psychophysical clinical one, showed a high repeatability as seen in Fig. 6(a) and Fig. 7(a). Moreover, although good correlation between the two types of measurement was observed, agreement was found to be low (see Fig. 8(b)). In order to correctly evaluate the agreement between the two methods, one must consider the way the different methods assess the MPOD. The proposed optical instrument, averages the total reflected light for the given field, as seen in equation 2. For the psychophysical instrument, on the other hand, it has been suggested that the measured MPOD is not that of the test field but rather the MPOD at its edge [10]. This could explain the low agreement (but high correlation) between the two instruments.

Reflectometric methods can often lead to an underestimation of MPOD due to scattering [18]. This underestimation can be as high as 16% depending on the amount of straylight in the eye. Using the previously presented formalism [18] we calculated that the contribution of the narrow annulus employed in the present work would have only minuscule effect on the measured MPOD. Although it is possible to measure straylight and take it into account for MPOD calculation, this is beyond the scope of this work.

Finally, each instrument suffers from different types of statistical errors: the psychophysical instrument, apart from the human factor, i.e. the subject's failure to properly decide on the flicker frequency, it also uses a fix amount of luminance green-blue ratios and therefore the accuracy of the measurement depends directly on this amount. At an MPOD level the different luminance ratios correspond to an accuracy of 0.05 D.U.. The proposed optical instrument, depends, too, on the human factor but to a lesser extend; the subject needs to fixate correctly and maintain this fixation throughout the 0.275 seconds of the measurement. Failure to do so could lead to an underestimation of the MPOD value as seen in the BA plot in Fig. 6(a). From a total of 147 measurements the largest error that was observed was 0.06D.U. which was attributed to bad fixation. Thermal noise or LED wavelength shift do not affect the measurement, due to its very short duration. That was, indeed, verified on an artificial eye. Other sources of error are blood vessels and reflections taking place mainly at the ILM in the periphery. The effect of blood vessels is minimal due to the large annular area considered and the fact that hemoglobin absorption is very similar for the chosen wavelengths. Reflections are largely wavelength independent, as verified by the fundus images acquired by the CMOS camera of the system and contribute little to the total signal detected.

## 5. Conclusion

In this work we proposed and validated an optical instrument for the assessment of the optical density of macular pigment. The objective was to have an accurate, easy-to-use, non-midriatic and potentially low-cost instrument which could potentially be used in clinical practice. The optical density of macular pigment was measured for 13 healthy volunteers; the system showed good repeatability and significant correlation with a commercially available psychophysical device.

## Funding

European Research Council (ERC) (AdG-2013-339228 SEECAT); Secretaría de Estado e Investigación, Desarrollo e Innovación (SEIDI) (FIS2013-41237-R); Fundación Séneca Agencia de Ciencia y Tecnología de la Región de Murcia (19897/GERM/15).

## Disclosures

The authors declare that there are no conflicts of interest related to this article.

## References

1. D. M. Snodderly, J. D. Auran, and F. C. Delori, "The Macular Pigment II. Spatial Distribution in Primate Retinas," *Investig. Ophthalmol. Vis. Sci.* **25**, 674–685 (1984).
2. E. Loane, C. Kelliher, S. Beatty, and J. M. Nolan, "The rationale and evidence base for a protective role of macular pigment in age-related maculopathy," *The Br. J. Ophthalmol.* **92**, 1163–1168 (2008).
3. K. Izumi-Nagai, N. Nagai, K. Ohgami, S. Satofuka, Y. Ozawa, K. Tsubota, K. Umezawa, S. Ohno, Y. Oike, and S. Ishida, "Macular pigment lutein is antiinflammatory in preventing choroidal neovascularization," *Arter. Thromb. Vasc. Biol.* **27**, 2555–2562 (2007).
4. S. Beatty, M. Boulton, D. Henson, H.-H. Koh, and I. J. Murray, "Macular pigment and age related macular degeneration," *Br. J. Ophthalmol.* **83**, 867–877 (1999).
5. J. Nolan and S. Beatty, "The role of macular pigment in the defence against AMD," *Optom. Today* **27**, 39–41 (2003).
6. B. R. Wooten and B. R. Hammond, "Macular pigment: Influences on visual acuity and visibility," *Prog. Retin. Eye Res.* **21**, 225–240 (2002).

7. J. Loughman, P. a. Davison, J. M. Nolan, M. C. Akkali, and S. Beatty, "Macular pigment and its contribution to visual performance and experience," *J. Optom.* **3**, 74–90 (2010).
8. P. Charbel Issa, R. L. van der Veen, A. Stijfs, F. G. Holz, H. P. Scholl, and T. T. Berendschot, "Quantification of reduced macular pigment optical density in the central retina in macular telangiectasia type 2," *Exp. Eye Res.* **89**, 25–31 (2009).
9. S. Müller, P. Charbel Issa, T. F. Heeren, S. Thiele, F. G. Holz, and P. Herrmann, "Macular Pigment Distribution as Prognostic Marker for Disease Progression in Macular Telangiectasia Type 2," *Am. J. Ophthalmol.* **194**, 163–169 (2018).
10. J. S. Werner, S. K. Donnelly, and R. Kliegl, "Aging and human macular pigment density," *Vis. Res.* **27**, 257–268 (1987).
11. B. R. Wooten, B. R. Hammond, R. I. Land, and D. M. Snodderly, "A practical method for measuring macular pigment optical density," *Investig. Ophthalmol. Vis. Sci.* **40**, 2481–2489 (1999).
12. L. T. Sharpe, A. Stockman, H. Knau, and H. Jägle, "Macular pigment densities derived from central and peripheral spectral sensitivity differences," *Vis. Res.* **38**, 3233–3239 (1998).
13. R. A. Bone and J. T. Landrum, "Heterochromatic flicker photometry," *Arch. Biochem. Biophys.* **430**, 137–142 (2004).
14. J. D. Moreland, "Macular pigment assessment by motion photometry," *Arch. Biochem. Biophys.* **430**, 143–148 (2004).
15. T. T. J. M. Berendschot and D. Van Norren, "Objective determination of the macular pigment optical density using fundus reflectance spectroscopy," *Arch. Biochem. Biophys.* **430**, 149–155 (2004).
16. A. O'Brien, C. Leahy, and C. Dainty, "Imaging system to assess objectively the optical density of the macular pigment in vivo," *Appl. Opt.* **52**, 6201–6212 (2013).
17. G. A. Fishman, P. E. Kilbride, K. R. Alexander, M. Fishman, and G. A. Fishman, "Macular Pigment Assessed By Imaging Fundus Reflectometry," *Vis. Res.* **29**, 663–674 (1989).
18. D. Christaras, A. Pennos, H. Ginis, and P. Artal, "Effect of intraocular scattering in macular pigment optical density measurements," *J. Biomed. Opt.* **23**, 1 (2018).
19. F. C. Delori, D. G. Goger, B. R. Hammond, D. M. Snodderly, and S. A. Burns, "Macular pigment density measured by autofluorescence spectrometry: comparison with reflectometry and heterochromatic flicker photometry," *J. Opt. Soc. Am. A* **18**, 1212–1230 (2001).
20. P. S. Bernstein, D. Y. Zhao, M. Sharifzadeh, I. V. Ermakov, and W. Gellermann, "Resonance Raman measurement of macular carotenoids in the living human eye," *Arch. Biochem. Biophys.* **430**, 163–169 (2004).
21. R. De Kinkelder, R. L. P. Van Der Veen, F. D. Verbaak, D. J. Faber, T. G. van Leeuwen, and T. T. J. M. Berendschot, "Macular pigment optical density measurements: evaluation of a device using heterochromatic flicker photometry," *Eye* **25**, 105–112 (2011).
22. J. Loughman, G. Scanlon, J. M. Nolan, V. O'Dwyer, and S. Beatty, "An evaluation of a novel instrument for measuring macular pigment optical density: the MPS 9000," *Acta Ophthalmol.* **90**, 90–97 (2012).
23. P. G. Davey, S. D. Alvarez, and J. Y. Lee, "Macular pigment optical density: Repeatability, intereye correlation, and effect of ocular dominance," *Clin. Ophthalmol.* **10**, 1671–1678 (2016).
24. J. Santamaría, P. Artal, and J. Bescós, "Determination of the point-spread function of human eyes using a hybrid optical-digital method," *J. Opt. Soc. Am. A, Opt. Image Sci.* **4**, 1109–1114 (1987).
25. P. Artal, "Optics of the eye and its impact in vision: a tutorial," *Adv. Opt. Photonics* **6**, 340–367 (2014).
26. H. Ginis, G. M. Pérez, J. M. Bueno, and P. Artal, "The wide-angle point spread function of the human eye reconstructed by a new optical method," *J. Vis.* **12**, 1–10 (2012).
27. D. Christaras, H. Ginis, and P. Artal, "Spatial properties of fundus reflectance and red - green relative spectral sensitivity," *J. Opt. Soc. Am. A* **32**, 1723–1728 (2015).
28. D. Christaras, H. Ginis, A. Pennos, and P. Artal, "Intraocular scattering compensation in retinal imaging," *Biomed. Opt. Express* **7**, 3996–4006 (2016).
29. D. Christaras, H. Ginis, A. Pennos, and P. Artal, "Scattering contribution to the double-pass PSF using Monte Carlo simulations," *Ophthalmic Physiol. Opt.* **37**, 342–346 (2017).
30. D. Christaras, "Light scattering phenomena in vision and in imaging," Ph.D. thesis, Universidad de Murcia (2016).
31. H. Ginis, O. Sahin, A. Pennos, and P. Artal, "Compact optical integration instrument to measure intraocular straylight," *Biomed. Opt. Express* **5**, 3036 (2014).
32. F. C. Delori, R. H. Webb, and D. H. Sliney, "Maximum permissible exposures for ocular safety (ANSI 2000), with emphasis on ophthalmic devices," *J. Opt. Soc. Am. A, Opt. Image Sci. Vis.* **24**, 1250–1265 (2007).
33. B. R. Hammond and K. Fuld, "Interocular differences in macular pigment density," *Investig. Ophthalmol. Vis. Sci.* **33**, 350–355 (1992).
34. J. J. Weiter, F. C. Delori, G. L. Wing, and K. A. Fitch, "Retinal pigment epithelial lipofuscin and melanin and choroidal melanin in human eyes," *Investig. Ophthalmol. Vis. Sci.* **27**, 145–152 (1986).
35. S. Y. Schmidt and R. D. Peisch, "Melanin concentration in normal human retinal pigment epithelium. Regional variation and age-related reduction," *Investig. Ophthalmol. Vis. Sci.* **27**, 1063–1067 (1986).
36. R. L. P. Van Der Veen, T. T. J. M. Berendschot, F. Hendrikse, D. Carden, M. Makridaki, and I. J. Murray, "A new desktop instrument for measuring macular pigment optical density based on a novel technique for setting flicker thresholds," *Ophthalmic Physiol. Opt.* **29**, 127–137 (2009).
37. J. van de Kraats, T. T. J. M. Berendschot, S. Valen, and D. Van Norren, "Fast assessment of the central macular

- pigment density with natural pupil using the macular pigment reflectometer,” *J. Biomed. Opt.* **11**, 064031 (2006).
38. F. C. Delori, “Autofluorescence method to measure macular pigment optical densities fluorometry and autofluorescence imaging,” *Arch. Biochem. Biophys.* **430**, 156–162 (2004).
  39. A. G. Robson, J. D. Moreland, D. Pauleikhoff, T. Morrissey, G. E. Holder, F. W. Fitzke, A. C. Bird, and F. J. G. M. Van Kuijk, “Macular pigment density and distribution: Comparison of fundus autofluorescence with minimum motion photometry,” *Vis. Res.* **43**, 1765–1775 (2003).
  40. T. T. J. M. Berendschot and D. Van Norren, “Macular pigment shows ringlike structures,” *Investig. Ophthalmol. Vis. Sci.* **47**, 709–714 (2006).
  41. M. L. Kirby, M. Galea, E. Loane, J. Stack, S. Beatty, and J. M. Nolan, “Foveal anatomic associations with the secondary peak and the slope of the macular pigment spatial profile,” *Investig. Ophthalmol. Vis. Sci.* **50**, 1383–1391 (2009).
  42. M. L. Kirby, S. Beatty, E. Loane, M. C. Akkali, E. E. Connolly, J. Stack, and J. M. Nolan, “A central dip in the macular pigment spatial profile is associated with age and smoking,” *Investig. Ophthalmol. Vis. Sci.* **51**, 6722–6728 (2010).
  43. I. Ctori and B. Huntjens, “The association between foveal morphology and macular pigment spatial distribution: An ethnicity study,” *PLoS ONE* **12**, 1–13 (2017).